Supporting Information

Chong et al. 10.1073/pnas.1003023107

SI Text

Smurf2 WW2 Does not Significantly Stabilize the WW3 Domain. To study whether stabilization of the WW3 by the WW2 also contributes to the enhancement in affinity observed when WW2 and WW3 are in tandem, thermal unfolding of the tandem WW23 and of a protein composed of the linker between the WW domains and the WW3 (linker-WW3) was monitored by CD spectroscopy (Fig. S4 *a* and *b*). The linker was included to isolate the effect of the WW2 domain on the interaction. NMR spectra suggest that the linker modestly enhances WW3 domain stability, implying that the linker enhances binding of S7PY. However, fluorescence experiments did not show that the linker-WW3 binds with significantly greater affinity to S7PY (Table S1), indicating that the linker does not account for the high S7PY affinity in the presence of the WW2. The CD thermal melts indicate that linker-WW3 has a thermal unfolding midpoint (Tm) of 47.9± 1.5 °C and 46.6 ± 1.5 °C in the absence and presence of S7PY, respectively. The WW2 is less stable and has a melting temperature of 36.1 ± 1.5 °C. The WW23 appears to undergo a single cooperative transition during thermal melting, with a Tm of 42.4 ± 1.5 °C. This could represent cooperative unfolding of the coupled WW23 or an overlay of WW2 and WW3 unfolding transitions. If the transition corresponds to melting of the coupled WW23 domain, then the data show that the WW2 does not substantially stabilize the WW3, but rather slightly destabilizes the WW3. The observed transition could also correspond to an overlay of independent WW2 and WW3 melting transitions, with the observed Tm being roughly the average of the WW2 and WW3 Tm values. In this case, the WW2-WW3 interaction is unstable leading to the conclusion that the WW2 does not significantly stabilize the WW3. Interestingly, the WW23-S7PY complex undergoes a single cooperative transition with a melting temperature of 52.7 ± 1.5 °C, indicating that the peptide significantly stabilizes the WW2, or the WW3, or both. Thus the CD data indicate that the WW2 does not lead to a significant stabilization of the WW3, does not enhance the Smurf2 interaction with S7PY by stabilizing the WW3, and may slightly destabilize the WW3.

To assess whether the tandem WW2 and WW3 domains interact in the absence of S7PY, we recorded HSQC spectra of the WW23 in the absence of the peptide. Spectra of the unbound Smurf2 WW23 are severely broadened, likely reflecting exchange between multiple conformations and/or aggregation (Fig. S2*b*). Less than half of the expected peaks are visible, and these occur in the disordered region of the HSQC. Comparison of spectra for unbound WT and C293A, a linker mutant, enables mapping of a portion of these peaks to the inter-WW domain linker. The chemical shifts indicate that the linker is more flexible in the absence of S7PY, implying that the WW2 and WW3 coupling with its associated restriction in linker flexibility is not constitutive. These data suggest that in the unbound state the WW23 may exchange between coupled and uncoupled WW domain conformations implying that the WW2 does not significantly stabilize the WW3 domain.

NMR was also used to study the effect of the WW2 on the stability of the isolated WW3 domain. Thermal melts of Smurf2 linker-WW3 were monitored by NMR (Fig. S4*c*). Increasing temperature caused the peaks to became progressively less dispersed in the amide proton dimension, moving from folded amide proton values to values that are characteristic of random coil. As for the WW2, the movement from folded values to random coil values indicates that the WW3 domain rapidly exchange between a folded and an unfolded state and that the WW3 is not fully folded even at 10 °C. When unlabeled Smurf2 WW2 was added to N^{15} labeled linker-WW3, several peaks in the HSQC shifted, indicating that the WW2 binds to the WW3, although the nature of the observed interaction is unclear. Fitting the peak movements using a standard binding equation yields an approximate dissociation constant of 1 mM at 25 °C (Fig. S4*d* and Table S1). Conservative estimates suggest that the linker-WW3 is at least 30% bound at the highest concentration of WW2. Thus if the WW2 is able to stabilize the WW3 *in trans* some evidence of stabilization should be observed at the highest concentrations of WW2. However, the chemical shift changes observed upon thermal stabilization (i.e., cooling) of the linker-WW3 are not duplicated by addition of the WW2. Thus the NMR data provides evidence that the WW2 does not stabilize the WW3 when added *in trans*.

SI Methods.

Protein and Peptide Preparation. DNAs encoding the Smurf2 WW2 and WW3 domains in tandem (Smurf2 WW23, aa 250–333), the Smurf1 interWW domain linker and WW2 domain (Smurf1 linker-WW2, aa 294–342), the Smurf1 WW2 domain (Smurf1 WW2, aa 306–342), and the PY-motif-containing regions of Smad1 and Smad2 (S1PY—Smad1, aa 215–236; S2PY—Smad2, aa 214–233) were amplified using PCR and inserted into pGEX 6P1 (GE Healthcare) using BamH1 and Xho1 restriction sites. DNAs encoding a long and short form of the Smurf1 WW1 and WW2 domains in tandem (Long Smurf1WW12, aa 234–342; Short Smurf1 WW12, aa 234–268 and 294–342) were amplified using PCR and inserted into linearized pET Small Ubiquitin-like Modifier (SUMO) vector (Invitrogen). A C293A mutant of Smurf2 WW23 was prepared by site-directed mutagenesis, using a QuikChange kit (Stratagene). A DNA encoding the Smurf2 inter-WW domain linker and WW3 domain (Smurf2 linker-WW3, aa 285–333) in pGEX 6P1 was produced by GenScript. All plasmid constructs were confirmed by sequencing. Polypeptides corresponding to the Smurf2 WW2 (Smurf2 WW2, aa 250–288) and WW3 domains (Smurf2 WW3, aa 297–333) and Smad7 PY motif region (S7PY, Smad7 aa 203–217) were prepared as previously described (1). The protein purification scheme for Smurf2 WW23, Smurf1 linker-WW2, and Smurf1 WW2 was identical to that previously described for Smurf2 WW2 and Smurf2 WW3 (1). Recombinant peptides corresponding to the PY-motif-containing regions of Smad1 and Smad2 were purified as described for the recombinant S7PY (1). Peptides corresponding to the PY-motif-containing regions of Smad1, Smad2, and Smad7 were also prepared using standard Fmoc chemistry by the Advanced Protein Technology Center at the Hospital for Sick Children. The peptides were purified as previously described (1). Long and Short Smurf1 WW12 were expressed in BL21 Codon Plus cells and induced for 16 h at 16 °C. Cells were lyzed in buffer containing 20 mM Na_2HPO_4, pH 7.5, 500 mM NaCl, 40 mM imidazole, and 2 mM DTT. The soluble fraction was loaded onto HisTrap columns (GE Healthcare) and eluted with 400 mM imidazole after washing the column with 10 column volumes of lysis buffer. After elution ULP protease (catalytic domain of Ubiquitin Like Protein specific protease 1) was added to cleave off the His-SUMO tag, and the sample was simultaneously dialyzed into 20 mM Tris HCl, pH 8.0, 200 mM NaCl, 2 mM DTT, and 5 mM imidazole. The cleaved protein was then loaded onto the HisTrap column again to remove the His-SUMO tag. The protein was then concentrated and purified by gel filtration using a Super-

dex75 column (GE Healthcare). Protein concentrations were determined by measuring their absorbance in 6 M GdnHCl using calculated extinction coefficients. Peptide concentrations were determined by amino acid analysis.

NMR Spectroscopy. Experiments were performed on a Varian INOVA 500-MHz spectrometer equipped with a pulsed field gradient unit and a triple resonance probe. Experiments were performed at 25 °C in buffer containing 40 mM Na_2HPO_4, pH 7.2, 20 mM NaCl, 1 mM EDTA, 0.05% NaN_3, 0.5 mM benzamidine and 10% D_2O, unless otherwise stated. Standard experiments were used to assign the backbone and side-chain resonances (2) of both Smurf2 WW23 and the S7PY peptide in the bound state, using a sample in which both polypeptides were ^{15}N and ^{13}C labeled. Short Smurf1 linker-WW2:S7PY and Short Smurf1 WW12:S7PY assignments were made by transferring assignments from Smurf2 WW3:S7PY and Smurf2 WW23:S7PY, respectively. To obtain NOE data for the complex we recorded a CN-NOESY-HSQC (3) spectrum with a mixing time of 120 ms. After initial assignment of ~1,000 NOEs, for which symmetry-related peaks were observed, ARIA1.2 (4) was used to facilitate the assignment of the remaining NOEs. TALOS (5) dihedral angle restraints were determined and used for structure calculations with errors set to the greater of 2 standard deviations or 20°. Residual dipolar coupling (RDC) restraints (6) were collected for the amide bonds using Pf1 phage alignment media (7). An alignment tensor was calculated (8) and subsequently refined using calculated structures and the program Module (9). NOE, TALOS, and RDC data and H-bond restraints were then input into CNS and used to calculate 200 structures. The 30 lowest energy structures were used for analysis by PROCHECK (10). Structures calculated without the H-bond restraints were almost identical. Heteronuclear NOE experiments (11) were recorded on a ^{15}N-labeled sample of Smurf2 WW23 and S7PY. Ribbon diagrams of molecular structures were generated using Molmol software (12).

Binding Studies. Fluorescence binding experiments were performed at 20 °C using an ATF105 AVIV Ratio spectrofluorometer with a Microlab 500 automated titrator. Proteins were dialyzed into filtered, degassed, and argon-purged buffers containing 40 mM Na_2HPO_4, pH 7.2, and 20 mM NaCl. 1 mM β-mercaptoethanol was added to the protein samples immediately before use. Fluorescence levels were monitored as peptide was added to the WW23 protein samples using an excitation wavelength of 295 nm and an emission wavelength of 333 nm. Data was fit as previously published (1). The temperature difference between sample in the fluorometer cell and titrant in the titrator had a negative effect on the precision of the results, which was corrected by subtracting a blank run in which WW23 protein without PY peptide was injected into a solution containing WW23 domain at the same concentration. Measurements were performed in duplicate or triplicate.

CD Spectroscopy Methods. Experiments were performed on a JASCO J-810 spectropolarimeter equipped with Peltier thermoregulation. Experiments were performed in buffer containing 40 mM Na_2HPO_4, pH 7.2, 20 mM NaCl, and 1 mM freshly added DTT using a 1-mm path length cell (Quartz-Suprasil, Hellma). Thermal unfolding was measured at least twice at wavelengths of 223 or 230 nm, with temperatures ranging from 2 to 95 °C. Raw data were fit to the following equation (13):

$$f(T) = ((I_N + S_N T) + (I_D + S_D T) \times \exp(-\Delta G_{D\text{-}N}(T)/RT))/(1 + \exp(-\Delta G_{D\text{-}N}(T)/RT)),$$

where I_N and I_D are the extrapolated signal for the native and denatured state at 0 K, S_N and S_D are the slopes of the native and denatured state baselines, T is the temperature in Kelvin, R is the ideal gas constant and $\Delta G_{D\text{-}N}$ is the free energy of unfolding, which is further described as

$$\Delta G_{D\text{-}N}(T) = \Delta H_{D\text{-}N}(1 - T/\mathrm{Tm}) + \Delta \mathrm{C}_{\mathrm{pD}\text{-}N}(T - \mathrm{Tm} - \mathrm{Tln}(T/\mathrm{Tm})),$$

where Tm is the midpoint of the thermal denaturation, $\Delta H_{D\text{-}N}$ is the enthalpy of denaturation at the midpoint, and $\Delta C_{\mathrm{pD}\text{-}N}$ is the heat capacity difference between the native and denatured state, which was estimated based on the protein size.

1. Chong PA, Lin H, Wrana JL, Forman-Kay JD (2006) An expanded WW domain recognition motif revealed by the interaction between Smad7 and the E3 ubiquitin ligase Smurf2. *J Biol Chem* 281:17069–17075.
2. Kanelis V, Forman-Kay JD, Kay LE (2001) Multidimensional NMR methods for protein structure determination. *IUBMB Life* 52:291–302.
3. Pascal S, Muhandiram DR, Yamazaki T, Forman-Kay JD, Kay LE (1994) Simultaneous acquisition of ^{15}N- and ^{13}C-edited NOE spectra of proteins dissolved in H20. *J Magn Reson Ser B* 103:197–201.
4. Nilges M (1998) Ambiguous NOEs and automated NOE assignment. *Prog Nucl Magn Reson Spectrosc* 32:107–139.
5. Cornilescu G, Delaglio, F, Bax A (1999) Protein backbone angle restraints from searching a database for chemical shift and sequence homology. *J Biomol NMR* 13:289–302.
6. Ottiger M, Delaglio F, Bax A (1998) Measurement of J and dipolar couplings from simplified two-dimensional NMR spectra. *J Magn Reson* 131:373–378.
7. Hansen MR, Mueller L, Pardi A (1998) Tunable alignment of macromolecules by filamentous phage yields dipolar coupling interactions. *Nat Struct Biol* 5:1065–v74.
8. Clore GM, Gronenborn AM, Bax A (1998) A robust method for determining the magnitude of the fully asymmetric alignment tensor of oriented macromolecules in the absence of structural information. *J Magn Reson* 133:216–221.
9. Dosset P, Hus JC, Marion D, Blackledge M (2001) A novel interactive tool for rigid-body modeling of multi-domain macromolecules using residual dipolar couplings. *J Biomol NMR* 20:223–231.
10. Laskowski RA, Rullmannn JA, MacArthur MW, Kaptein R, Thornton JM (1996) AQUA and PROCHECK-NMR: Programs for checking the quality of protein structures solved by NMR. *J Biomol NMR* 8:477–486.
11. Kay LE, Torchia DA, Bax A (1989) Backbone dynamics of proteins as studied by ^{15}N inverse detected heteronuclear NMR spectroscopy: Application to staphylococcal nuclease. *Biochemistry* 28:8972–8979.
12. Koradi R, Billeter M, Wuthrich K (1996) MOLMOL: A program for display and analysis of macromolecular structures. *J Mol Graph* 14:51–55, 29–32.
13. Fersht AR (1999) *Structure and Mechanism in Protein Science* (Freeman, New York), pp 508–539.

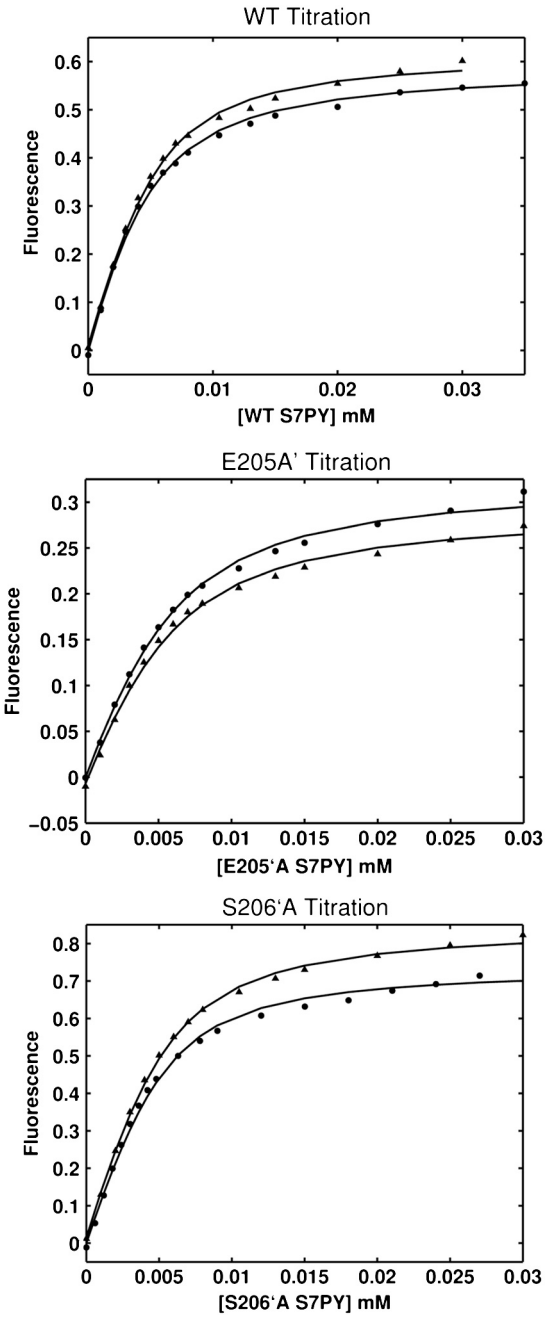

Fig. S1. Representative data and fits for titrations of WT, E205′A, and S206′A S7PY into Smurf2 WW23. Data and fits for two experiments are shown for each S7PY peptide. Data were fit as described in *SI Methods*. The dissociation constants for WT (triplicate measurements), E205′A (duplicate), and S206′A (duplicate) were 1.7 ± 0.4, 2.5 ± 0.2, and 1.6 ± 0.3 μM, respectively.

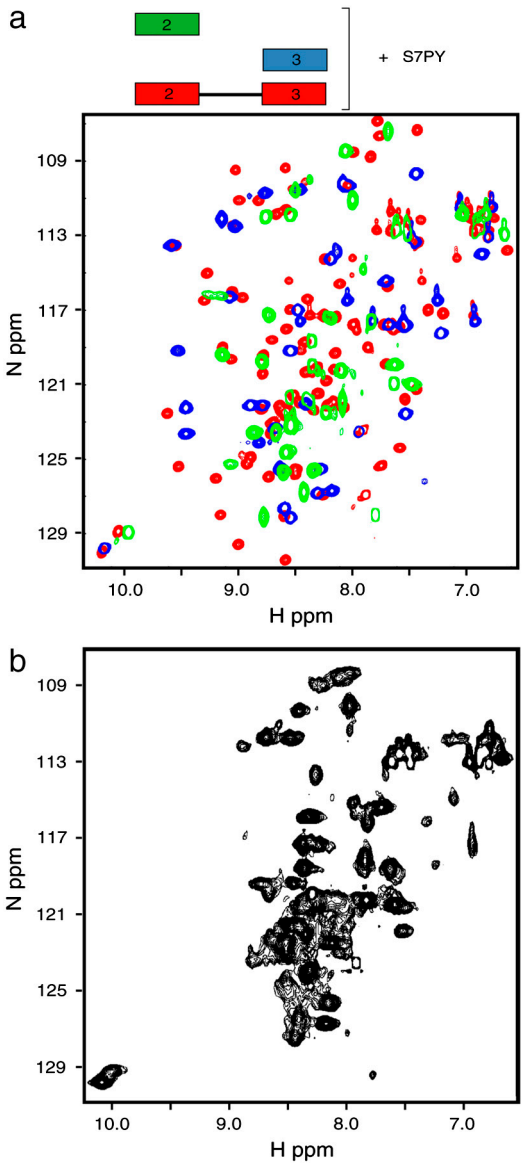

Fig. S2. (*a*) Tandem Smurf2 WW23 uses an altered binding mechanism compared to the isolated WW3 domain for recognition of S7PY. Superposition of Smurf2 WW2 (green), WW3 (blue), and WW23 (red) ^{1}H-^{15}N HSQC spectra recorded at 25 °C in the presence of S7PY peptide. (*b*) ^{1}H-^{15}N HSQC spectrum of apo Smurf2 WW23 recorded at 25 °C. Note the narrow amide proton dispersion, the broadness of the peaks and the limited number of peaks. Less than half of the expected number of peaks is observed.

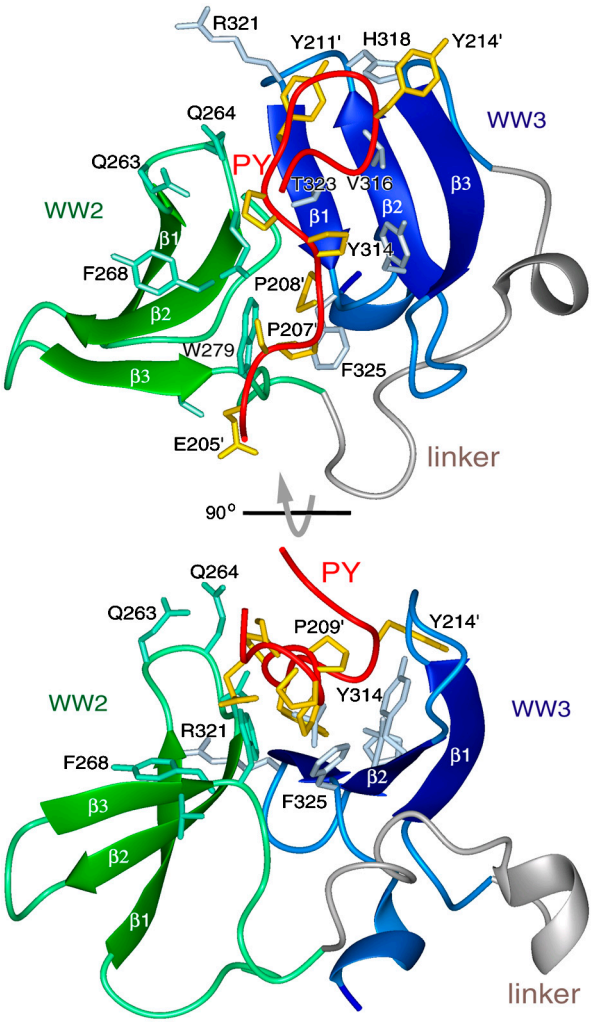

Fig. S3. Ribbon diagrams of the Smurf2 WW23:S7PY complex shown in two orientations, which differ by 90 °. The Smurf2 WW2 domain, the interdomain linker, and the WW3 domain are shown in green, gray, and blue, respectively. The backbone of the Smad7 PY motif-containing peptide S7PY is shown in red, whereas the side chains are in yellow. For clarity, only a fraction of the side chains is shown. Residues identified with the prime symbol correspond to Smad7 residues.

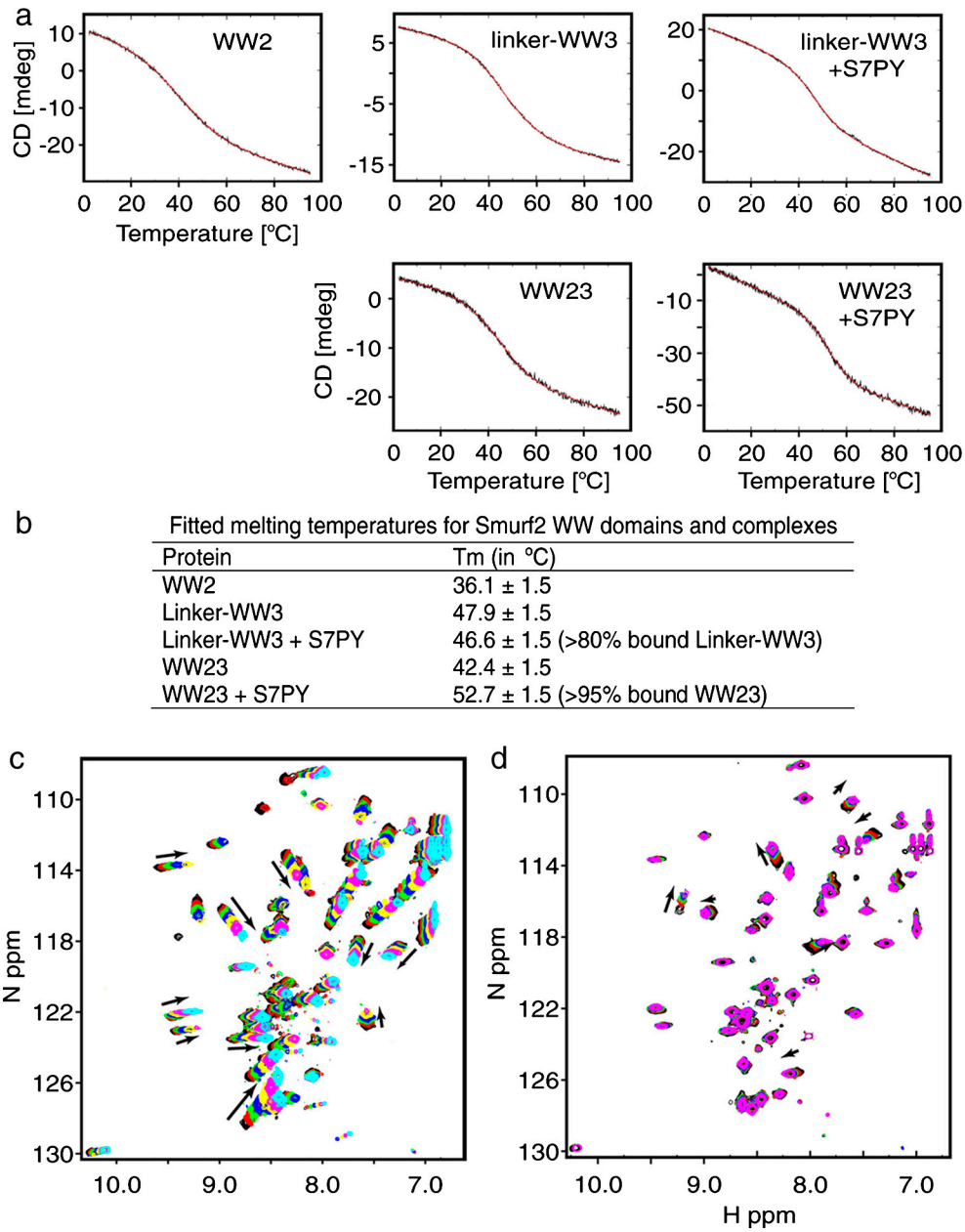

b

Fitted melting temperatures for Smurf2 WW domains and complexes

Protein	Tm (in °C)
WW2	36.1 ± 1.5
Linker-WW3	47.9 ± 1.5
Linker-WW3 + S7PY	46.6 ± 1.5 (>80% bound Linker-WW3)
WW23	42.4 ± 1.5
WW23 + S7PY	52.7 ± 1.5 (>95% bound WW23)

Fig. S4. (*a*) Representative CD monitored thermal melts of various Smurf2 WW domain constructs in the presence and absence of S7PY. Black lines represent the raw data, whereas the red lines represent the fit obtained using a standard two-state folding equation (see *SI Methods*). The CD melts were performed at least in duplicate. (*b*) Melting temperatures obtained by fitting the CD melts. The minimum error was set to 1.5 °C based on the largest observed standard deviation for this set of experiments. (*c*) Overlay of Smurf2 linker-WW3 ^{1}H-^{15}N HSQC spectra recorded at temperatures of 5 °C (black), 10 °C (red), 15 °C (green), 20 °C (blue), 25 °C (yellow), 30 °C (magenta), and 35 °C (cyan). The arrows indicate the direction of the peak movement with increasing temperature. (*d*) Overlay of Smurf2 linker-WW3 ^{1}H-^{15}N HSQC spectra recorded in the presence of increasing concentrations of WW2 domain. Ratios of WW2:WW3 are 0 (black), 0.49 (red), 0.92 (green), 1.42 (blue), and 2.09 (magenta). The arrows indicate the direction of the peak movement with increasing WW2.

a

```
          E205' S206'
Smad7   CELESPPPYSRY.PMDFLK
Smad6   CGPESPPPYSRLSPRDEYK
Smad1   MPADTPPPAYLPPEDPMTQD
Smad5   LPADTPPPAYMPPDDQMGQD
Smad2   YIPETPPPGYISEDGETSDQ
Smad3   NIPETPPPGYLSEDGETSDH
```

b

```
hsmurf1 WW1            235 ELPEGYEQRTTVQGQVYFLHTQTGVSTWHDPRI
hsmurf2 WW2            252 DLPEGYEQRTTQQGQVYFLHTQTGVSTWHDPRV
hWWP1 WW2              278 PLPPGWEKRVDSTDRVYFVNHNTKTTQWEDPRT
hWWP2 WW3              406 PLPPGWEKRQD-NGRVYYVNHNTRTTQWEDPRT
hItch WW3              398 PLPPGWEKRTDSNGRVYFVNHNTRITQWEDPRS
hWWP2 WW1              301 ALPAGWEQRELPNGRVYYVDHNTKTTTWER---
hItch WW1              286 PLPPGWEQRVDQHGRVYYVDHVEKRTTWDRPE-
hNedd4 WW3             422 FLPKGWEVRHAPNGRPFFIDHNTKTTTWEDPRL
hNedd4l WW3            377 FLPPGWEMRIAPNGRPFFIDHNTKTTTWEDPRL

hsmurf1 long linker    268 PSPSGTIPGGDAAFLYEFLLQGHTSEPRDLNSVNCDELG
hsmurf1 short linker   294 -------------------------PRDLNSVNCDELG
hsmurf2 WW2-3 linker   285 -------------------------PRDLSNINCEELG
hWWP1 WW2-3 linker     311 ------------------------------QGLQNEE--
hWWP2 WW3-4 linker     438 ------------------------------QGMIQEP--
hItch WW3-4 linker     431 ------------------------------QGQLNEK--
hWWP2 WW1-2 linker         ---------------------------------------
hItch WW1-2 linker         ---------------------------------------
hNedd4 WW3-4 linker    455 --------------------KIPAHLRGKTSLDTSNDLG
hNedd4l WW3-4 link.    410 --------------------KFPVHMRSKTSLNP-NDLG

hsmurf1 WW2            307 PLPPGWEVRSTVSGRIYFVDHNNRTTQFTDPRL
hsmurf2 WW3            298 PLPPGWEIRNTATGRVYFVDHNNRTTQFTDPRL
hWWP1 WW3              318 PLPEGWEIRYTREGVRYFVDHNTRTTTFKDPRN
hWWP2 WW4              445 ALPPGWEMKYTSEGVRYFVDHNTRTTTFKDPRP
hItch WW4              438 PLPEGWEMRFTVDGIPYFVDHNRRTTTYIDPRT
hWWP2 WW2              331 PLPPGWEKRTDPRGRFYYVDHNTRTTTWQRPTA
hItch WW2              318 PLPPGWERRVDNMGRIYYVDHFTRTTTWQRPTL
hNedd4 WW4             474 PLPPGWEERTHTDGRIFYINHNIKRTQWEDPRL
hNedd4l WW4            428 PLPPGWEERIHLDGRTFYIDHNSKITQWEDPRL
```

Fig. S5. (*a*) Alignment of the PY-motif-containing regions of the Smad proteins. The E/D-S/T-P and PY motifs are highlighted in cyan and pink, respectively. (*b*) Alignment of a selection of WW domains and linkers from human HECT E3 ubiquitin ligases. The Smurf sequences are shown in bold.

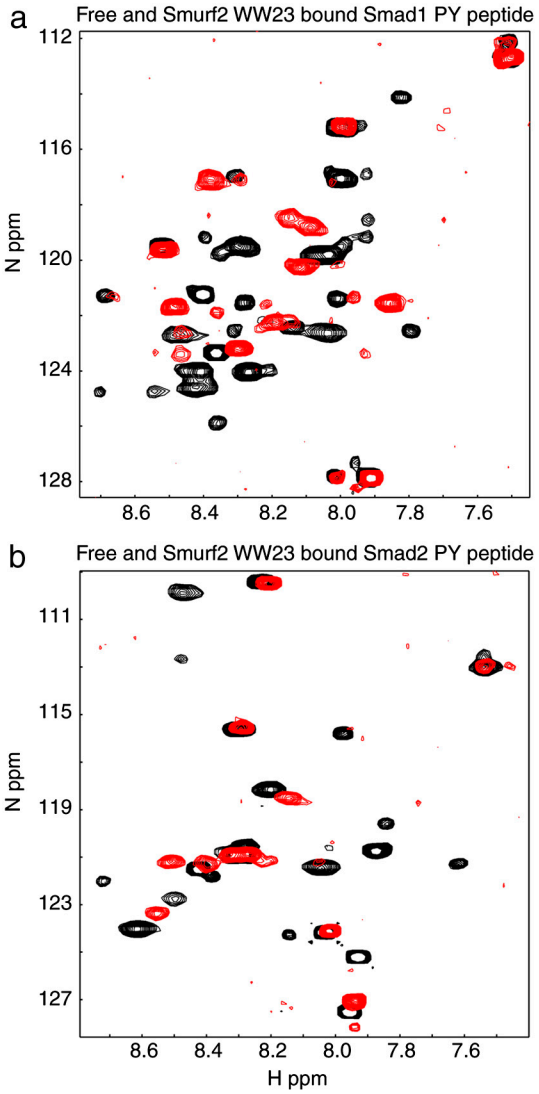

Fig. S6. (*a*) Overlay of HSQC spectra of a ^{15}N labeled Smad1 PY peptide in the free (black) and Smurf2 WW23 bound state (red). (*b*) Overlay of HSQC spectra of a ^{15}N labeled Smad2 PY peptide in the free (black) and Smurf2 WW23 bound state (red).

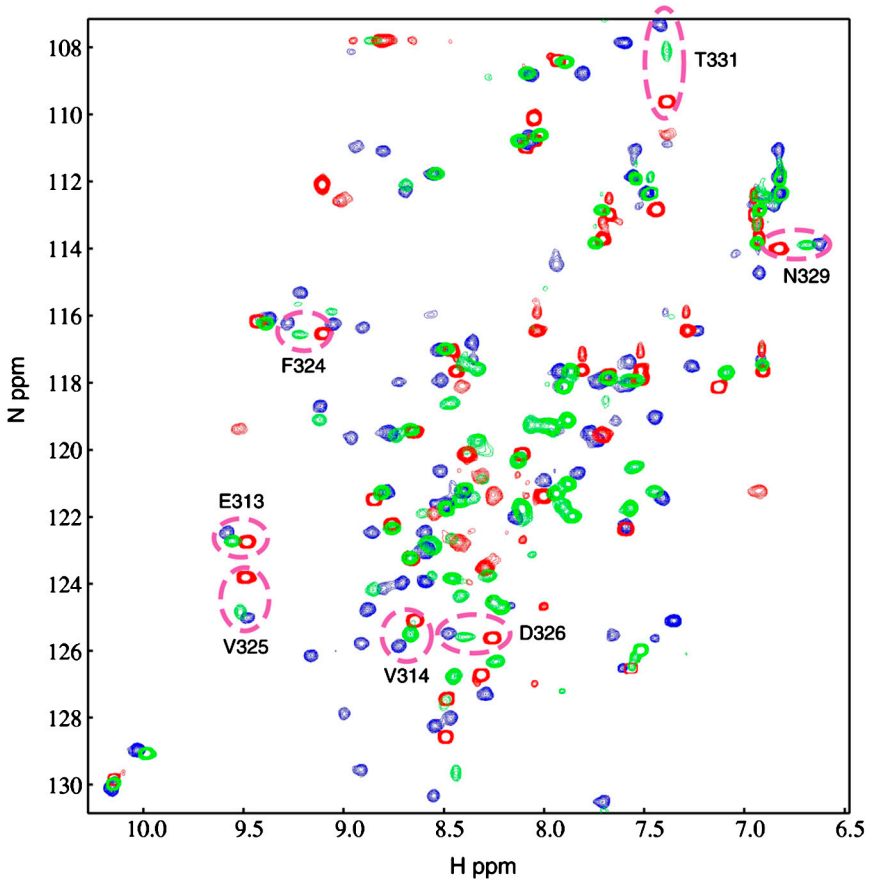

Fig. S7. The WW2 domain of Long Smurf1 WW12 binds to S7PY in both an independent and a WW1 bound format. Overlay of ^{1}H-^{15}N HSQC spectra of Short Smurf1 WW12:S7PY (blue), Short Smurf1 linker-WW2:S7PY (red), and Long Smurf1 WW12:S7PY (green) complexes. Peaks representing the same residues in the different complexes are circled and identified.

Table S1. Dissociation constants for various Smurf2 WW domain complexes measured by fluorescence spectroscopy*

Protein	Ligand	K_d, in μM
WW2	S7PY	Not detectable (by fluorescence or NMR)†
WW3	S7PY	40.0 ± 0.1†
Linker-WW3	S7PY	Between 10 and 300‡
WW23	S7PY	1.7 ± 0.4
WW23	S7PY E205′A	2.5 ± 0.2
WW23	S7PY S206′A	1.6 ± 0.3
Linker-WW3	WW2	∼1,000 (determined by NMR)

*Fluorescence experiments were performed at least in duplicate.
†See ref. 1.
‡The binding curves for linker-WW3 did not allow for a more precise fitting of the binding affinity.

Table S2. Structural Statistics for the 30 final structures of the Smurf2 WW23:S7PY Complex

rms deviations from restraints	**Number**	
Unambiguous and ambiguous NOEs (Å)	4,146	0.013 ± 0.001
WW2 to WW3 NOEs	72	
WW2 to S7PY	99	
WW3 to S7PY	138	
H bonds	20	
Dihedral angles (°)	56	0.43 ± 0.09
RDC restraints (Q^{free}) *	44	0.32 ± 0.02
rms deviations from idealized geometry		
Bonds (Å)		0.0033 ± 0.0001
Angles (°)		0.55 ± 0.02
Impropers (°)		0.48 ± 0.03
Ramachandran map: Smurf2 (250–286,292–331) & Smad7 (205′–217')		
Most favored regions		81.8 ± 2.7%
Additionally allowed regions		13.7 ± 3.1%
Generously allowed regions		2.7 ± 2.1%
Disallowed regions †		1.8 ± 1.3%
Atomic rmsd (Å) from mean structure	**Backbone**	**All heavy atoms**
Smurf2 (253–329), Smad7 (205′–216′)	0.74 ± 0.16	1.40 ± 0.16
Smurf2 WW2 (253–283)	0.48 ± 0.12	1.20 ± 0.16
Smurf2 WW3 (299–329)	0.39 ± 0.10	1.12 ± 0.13
Smad7 (205'–216')	0.85 ± 0.32	1.66 ± 0.42

*The quality factor, Q^{free} (1), was calculated by comparing the predicted RDCs from structures calculated without using the RDCs to the experimentally obtained values. If structures calculated using the RDCs are used to determine *Q*, the deviation is essentially zero.

†Residues in the disallowed regions occur in flexible regions where there is a paucity of data. These regions are found in different conformations in the members of the ensemble. In each case, these residues are in the disallowed region in a minor fraction of the ensemble. Residues in the disallowed regions of some structures include E205′ (flexible N-terminus of S7PY), S212′, R213′, D252, L253, E255, Q263.

1. Bax A, Grishaev A (2005) Weak alignment NMR: A hawk-eyed view of biomolecular structure. *Curr Opin Struct Biol* 15:563–570.